A Facile Electrochemical Method to Prepare Pt Disk Electrode with (100) Preferential Orientation for Investigating Structure-Sensitive Electro-Oxidation Reactions

Zhi Liu[1], Yao Yang[1], Baipo Shu[3,*], Jie Liu[2], Xu Chen[1], Yingbo Li[2], Yida Deng[2], Xiaopeng Han[2], Wenbin Hu[1,2], Cheng Zhong[2,*]
[1] State Key Laboratory of Metal Matrix Composites, Shanghai Jiao Tong University, Shanghai, 200240, China
[2] Key Laboratory of Advanced Ceramics and Machining Technology (Ministry of Education) and Tianjin Key Laboratory of Composite and Functional Material, Department of Materials Science and Engineering, Tianjin University, Tianjin 300072, China
[3] Faculty of Materials Science and Engineering, Kunming University of Science and Technology, Kunming 650093, China.
[*]E-mail: cheng.zhong@tju.edu.cn (C. Zhong); sbp20020@126.com (B.P. Shu)

A square-wave voltage was used to electrochemically treat the Pt disk electrode with 5 mm diameter in H_2SO_4 solution by a two-electrode cell. The surface preferential orientation of a Pt disk electrode can be controlled by the lower potential limit and the frequency of the square-wave voltage. The lower potential limit of –2.4 V and the frequency of 2000 Hz resulted in the formation of (100)-oriented Pt surface on the disk electrode. Hydrogen desorption profile suggested the significantly increased proportion of Pt(100) sites in the electrochemically treated Pt disk electrode. Four typical and important structure-sensitive electro-oxidation reactions were selected for investigating the electrocatalytic activity of Pt electrodes. Electrochemically treated Pt disk electrodes exhibited much higher specific activities for the electro-oxidation of ethanol and ammonia, and revealed lower specific activity for formic acid electro-oxidation, which agrees well with previous studies on Pt(100) single crystal electrodes. The above results suggest that the electrochemical treatment method can be used as a very facile and one-step way to prepare model Pt disk electrode with well-defined (100) preferential surface orientation for the investigation of the structure-sensitive reactions.

1. INTRODUCTION

Platinum (Pt) has been extensively studied as a key electrocatalyst for a wide variety of important electrocatalysis applications, which play a significant role in energy conversion applications.

For example, Pt has been the most commonly studied electrocatalyst for electro-oxidation of methanol [1-3], ethanol [4-6], formic acid [7, 8], ammonia [9-13] and hydrazine [12]. The electro-oxidation reactions of ethanol and methanol plays a key role in direct alcohol-based fuel cells. The electro-oxidation of ammonia has recently attracted increasing interest since it addresses both clean energy supply free of greenhouse gas (CO_2) and environmental protections, as discussed by several reviews [9-12]. For example, Botte et al. [14-19] proposed that the electro-oxidation of ammonia could be used to produce high-purity hydrogen on board while simultaneously removing ammonia effluents in wastewater.

Since many chemical properties strongly depend on the surface atomic arrangements and thus the surface crystallographic plane of Pt, extensive studies have been carried out on Pt single crystal electrodes not only to investigate the relationship between the surface crystalline structure and the electrocatalytic property but also to guide the development of high-performance electrocatalysts [20, 21]. For example, using Pt single crystal electrodes with three different basal planes (Pt(111) and Pt(110) and Pt(100)), Vidal-Iglesias et al. [22] found that Pt(111) and Pt(110) single crystals showed a very small reactivity while Pt(100) single crystal exhibited a considerably high activity towards ammonia electro-oxidation. Marković et al. [23] reported that the activity of Pt(*hkl*) for oxygen reduction reaction in H_2SO_4 solution increased in the order of (111) < (100) < (110). Sun et al. [24] found that the electrocatalytic activity of Pt for electro-oxidation of formic acid was also dependent on the surface crystallographic plane of Pt, following the order of Pt(110) > Pt(111) > Pt(100).

Although Pt single crystal electrodes can provide definitive information about the relationship between the surface structure and the electrocatalytic activity of a certain reaction, it is experimentally difficult to prepare Pt single crystal electrodes especially to prepare it in a geometry for the use of disk electrode (RDE) [25-27]. The preparation of Pt single crystal electrodes generally requires complicated experimental procedures and equipment [25, 28]. Typical procedures include careful cutting and polishing to certain orientation, flame annealing and cooling in H_2, and also complicate pretreatment processes to obtain a well-defined surface. This sophisticated method for preparing Pt single crystal electrodes strongly limits the experimental research of various electro-oxidation reactions on well-defined Pt surfaces with certain orientation. Prof. Arvia's group [29-33] proposed a facile electrochemical faceting method to obtain Pt electrodes with preferential orientation. However, it has remained unclear whether this method can be used to prepare model electrode for the investigation of other structure-sensitive reactions such as electro-oxidation of ammonia, methanol, ethanol and formic acid.

In the present work, a simple two-electrode system was used to prepare Pt disk electrode with preferential orientation by high-frequency square-wave voltage. By controlling the frequency (*f*), upper (E_u) and lower potential (E_L) limits of the square-wave voltage, Pt disk electrode with (100) preferential orientation was obtained. The surface morphology of the electrochemically treated Pt electrode was characterized by the scanning electron microscopy (SEM). Several typical structure-sensitive reactions including electro-oxidation of methanol, ethanol, formic acid and ammonia were selected as model reactions to investigate the electrocatalytic activity of electrochemically treated Pt electrodes.

2. EXPERIMENTAL

2.1. Reagents and Materials

H_2SO_4, $(NH_4)_2SO_4$, methanol (CH_3OH), ethanol (C_2H_5OH) and formic acid (HCOOH) were purchased from Sinopharm Chemical Reagent Co., Ltd., and were of analytical grade. KOH ($\geq 85.0\%$) was obtained from Shanghai Lingfeng Chemical Reagent Co., Ltd. All reagents were used without further purification. The ultrapure water with the resistivity of 18.2 MΩ cm is obtained from Milli-Q water purification system. All the solutions in the electrochemical test were deaerated by bubbling a high-purity N_2 gas (99.999%).

2.2. Electrode Preparation and characterization

Prior to use, a Pt disk electrode (diameter = 5 mm, geometric surface area = 0.196 cm^2) was polished with 1, 0.3 and 0.05 μm alumina slurry sequentially and sonicated in ultrapure water to clean the surface. The electrochemical treatment of the Pt disk electrode was performed on a multifunction generator (WF1973, NF Corporation, Japan) coupled with power supply (BP4610, NF Corporation, Japan), using a two-electrode cell. The two electrodes were a Pt disk electrode and a graphite rod, respectively, and the solution was 1 M H_2SO_4. Periodic square-wave voltage with different values of f, E_u and E_L were used to treat the Pt disk electrode. The surface morphologies of the Pt disk electrode before and after the electrochemical treatment (square-wave voltage treatment) were recorded with the scanning electron microscopy (SEM, S-4800, Hitachi, Japan). The crystalline structure of the Pt disk electrode was characterized by an X-ray diffraction (XRD, BRUKER-AXS) using Cu K_α radiation (λ=0.15406 nm) at a scan rate of 2° min^{-1}.

2.3. Electrochemical measurements

Electrochemical measurements were performed in a classical three-electrode cell, with a PARSTAT 2273 electrochemical workstation. Untreated or electrochemically treated Pt disk electrode was used as the working electrode. A Pt plate and a saturated calomel electrode (SCE) were used as the counter electrode and the reference electrode, respectively. The electrochemically active surface area (ECSA) of the Pt disk electrode was determined by the hydrogen desorption charge obtained from the steady-state cyclic voltammograms (CVs) at a scan rate of 0.05 V s^{-1} in 0.5 M H_2SO_4 solution. The electrocatalytic activity for methanol oxidation of the Pt disk electrode was recorded with the CV measurement in 0.5 M H_2SO_4 + 0.5 M CH_3OH solution at a scan rate of 0.05 V s^{-1}. In the case of ethanol electro-oxidation, the CV measurement was performed in 0.5 M H_2SO_4 + 0.5 M C_2H_5OH solution at 0.05 V s^{-1}. For electro-oxidation of formic acid, the CV measurement was performed in 0.5 M H_2SO_4 + 0.5 M HCOOH solution at 0.05 V s^{-1}. The electro-oxidation of ammonia was carried out in 1 M KOH + 0.05 M $(NH_4)_2SO_4$ solution by CV at 0.01 V s^{-1}. In order to compare the intrinsic activity of the Pt disk electrode before and after electrochemical treatment, all the currents in the CV curves

were normalized by the ECSA of Pt. All electrochemical experiments were performed at controlled temperature of 25±1°C.

3. RESULTS AND DISCUSSION

Fig. 1 shows the CV measured on the untreated Pt disk electrode in 0.5 M H_2SO_4 solution. Typical cyclic voltammetric features of polycrystalline Pt in acid solution can be observed, which shows characteristic potential regions including the hydrogen adsorption/desorption region from −0.2 to 0.1 V(SCE), the double-layer region from −0.1 to 0.4 V(SCE) and the Pt oxidation/reduction region from 0.4 to 1.0 V(SCE) [34]. Hydrogen adsorption/desorption process is highly dependent on the surface structure of Pt and has been widely used as a fingerprint to characterize the type and density of surface sites on Pt [35-38]. The hydrogen desorption peaks at about −0.15 V(SCE) (h_1) and −0.05 V(SCE) (h_2) in the anodic branch of the CV are caused by the desorption of weakly and strongly bonded hydrogen species, which are related with Pt(110) sites and Pt(100) sites, respectively [35-37, 39]. For polycrystalline Pt, the value of h_2/h_1 is below 1 (typically about 0.9), which agrees well with the CV result in Fig. 1. Besides, the ECSA of Pt can also be estimated from the CV curves by [40]:

$$\mathrm{ECSA} = \frac{Q_H}{Q_H^0} \qquad (1)$$

where Q_H is the hydrogen desorption charge (mC cm^{-2}), and Q_H^0 is the specific charge for the formation of a hydrogen monolayer on the polycrystalline Pt (0.21 mC cm^{-2}) [41, 42]. The value of Q_H can be calculated by integrating the area corresponding to the hydrogen adsorption current after subtracting the double-layer contribution.
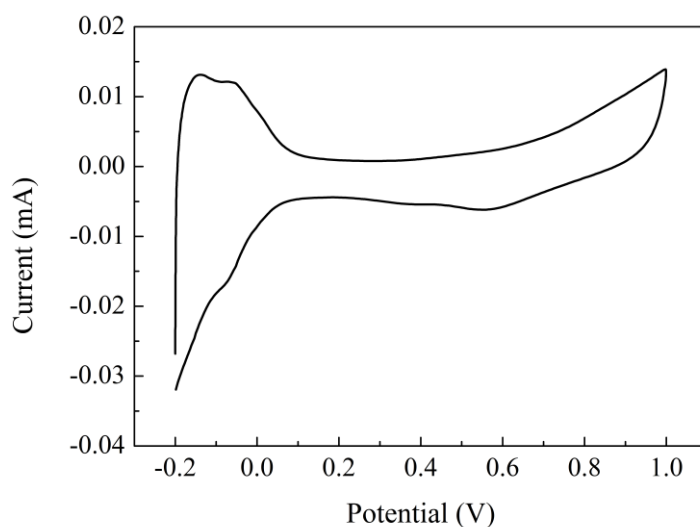

Figure 1. CV curve measured on the polished Pt disk electrode in 0.05 M H_2SO_4 solution at a scan rate of 0.05 V s^{-1}.

Fig. 2 shows CVs measured on Pt disk electrodes electrochemically treated at different E_L (the values of E_u and f of the square-wave voltage are 0.6 V and 400 Hz, respectively). For Pt disk

electrodes electrochemically treated at higher E_L (−1.9 and −2.1 V), the current peak density at −0.15 V(SCE) is higher than that at −0.05 V(SCE), which is the typical feature of polycrystalline Pt [36, 39]. As the E_L decreases to −2.3 and 2.5 V, the value of current peak at −0.05 V(SCE) obviously increases and its value is higher than the current peak value at −0.15 V(SCE). This is the characteristic feature of Pt with (100) preferential orientation, suggesting that the proportion of Pt (100) sites increases as the E_L decreases under the investigated range. In our previous work [38], we found that the enhanced hydrogen evolution with the decreasing of the electrode potential plays an important role in the increased proportion of Pt (100) sites in Pt nanoparticles. It is anticipated that similar mechanism is also applied for the surface reconstruction of the Pt disk electrode during the electrochemical treatment.
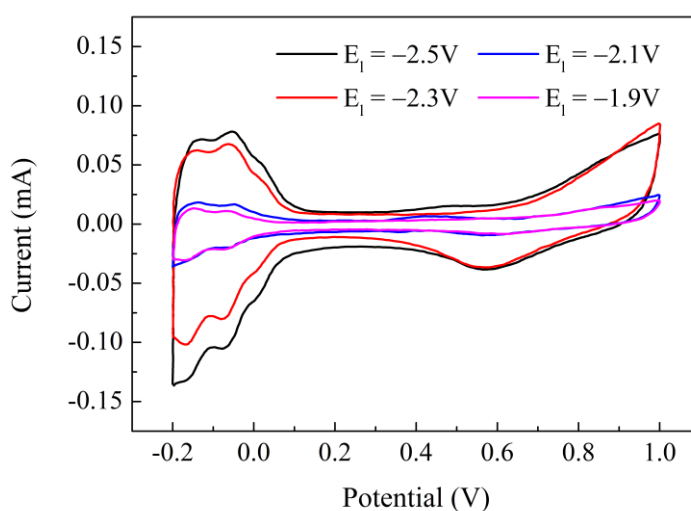

Figure 2. CVs measured on Pt disk electrodes electrochemically treated at different lower potential limit of square-wave voltage (CV scan rate: 0.05 V s^{-1}).

Fig. 3 shows CVs measured on Pt disk electrodes electrochemically treated at different f (the values of E_L and E_u of the square-wave voltage are −2.4 and 0.8 V, respectively). Depending on the condition of the electrochemical treatment, the hydrogen desorption region shows two or three characteristic peaks (i.e., h$_1$, h$_2$ and/or h$_3$) located at about −0.15, −0.05 and 0.02 V(SCE), corresponding to Pt(110) sites, Pt(100) steps and terrace borders and Pt(100) terrace or wide domains, respectively [35, 37, 43]. The frequency of the square-wave voltage (f) also plays a vital role in the hydrogen desorption profile of treated Pt disk electrodes. When f ranges from 500 and 2000 Hz, the current peak height of h$_1$ is lower than that of h$_2$ and there is a shoulder peak h$_3$. These are typical features of Pt with (100) surface orientation. However, as f further increases to 4000 Hz, the characteristic of CV is similar to that of polycrystalline Pt. Furthermore, hydrogen desorption profile shows the highest value of h$_2$/h$_1$ and the most obvious h$_3$ peak for the Pt disk electrode treated at 2000 Hz, indicating the largest Pt(100) fraction is obtained under this condition.
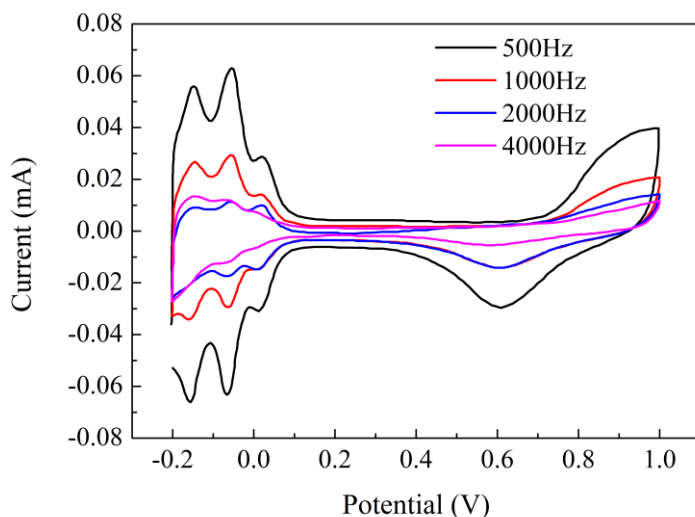
Figure 3. CVs measured on Pt disk electrodes electrochemically treated at different frequency of square-wave voltage (CV scan rate: 0.05 V s^{-1}).

Fig. 4a and b show SEM images of the Pt disk electrode before and after the electrochemical treatment ($f = 2000$ Hz, $E_L = -2.4$ V and $E_u = 0.8$ V). The inset in the figure shows the high-magnification SEM image. Before the electrochemical treatment, the Pt surface is relatively smooth with some shallow scratches introduced during the polishing procedure.
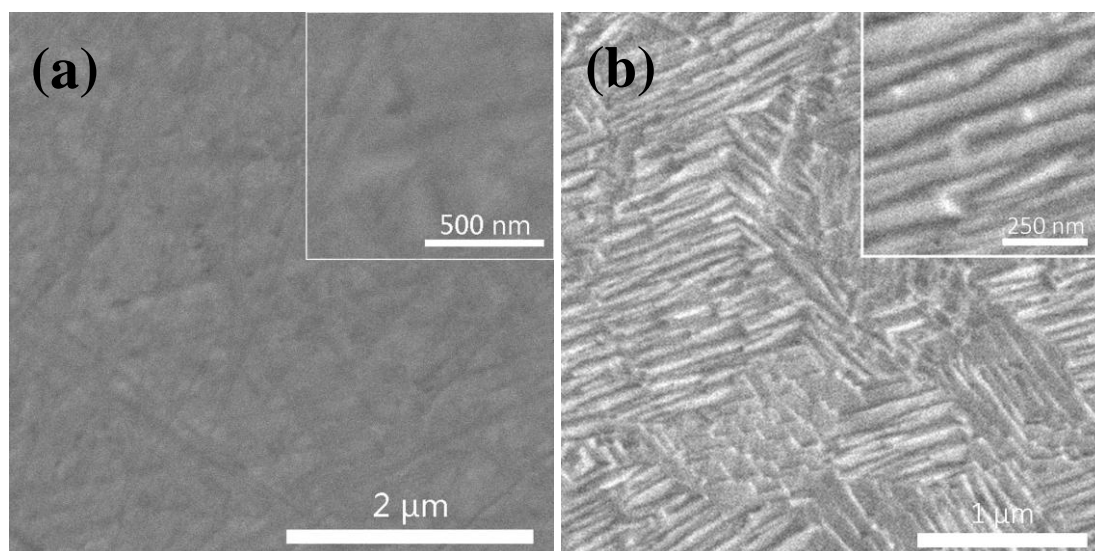

Figure 4. SEM images of (a) polished Pt disk electrode without the electrochemical treatment and (b) electrochemically treated Pt disk electrode ($f = 2000$ Hz, $E_L = -2.4$ V and $E_u = 0.8$ V).

The surface morphology of the Pt surface shows a dramatic change after the electrochemical treatment. The scratches on the original Pt surface disappear and the electrochemically treated Pt surface shows a highly stepped surface with parallel-terrace-like morphology. Grains and grain

boundaries can be clearly observed on the surface, and each grain exhibits a cuboid morphology with preferred orientation. This corresponds to the obvious change of the CV profile of the electrochemically treated Pt surface.

Fig. 5 shows the XRD patterns of the Pt disk electrode before and after the electrochemical treatment (f = 2000 Hz, E_L = −2.4 V and E_u = 0.8 V). Peaks around 39.6°, 46.2°, 67.4° and 81.2° correspond to diffraction peaks of crystal faces of Pt(111), Pt(200), Pt(220) and Pt(311), respectively. Generally, the intensity ratio of the height peak of Pt(200)/Pt(111) can be used to characterize the preferential degree of Pt(100). It is seen that there is no obvious change in the relative intensity ratio between Pt(200) and Pt(111) peak after the electrochemical treatment, and both XRD patters show typical polycrystalline structure without distinct preferential orientation [43]. In XRD measurements, the effective information depth of X-ray is generally large (typically larger than 10 μm). However, the preferentially oriented surface obtained by the electrochemical treatment is only located at the very surface of the Pt disk electrode (Fig. 4b) and therefore cannot be reflected by XRD measurements.
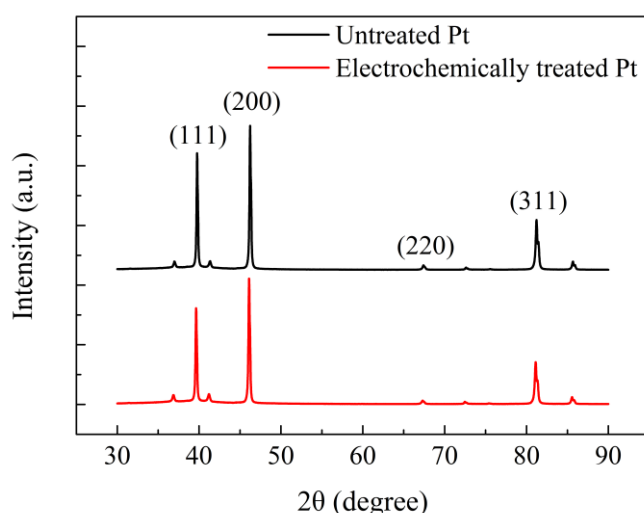

Figure 5. X-ray patterns of polished Pt disk electrode without the electrochemical treatment and electrochemically treated Pt disk electrode (f = 2000 Hz, E_L = −2.4 V and E_u = 0.8 V).

To better understand the effect of the electrochemical treatment on the preferential orientation of the Pt surface and thus the electrocatalytic activity, the electro-oxidation of methanol, ethanol, formic acid and ammonia has been selected for the investigation of typical structure-sensitive reactions. Fig. 6 shows CVs of the methanol electro-oxidation on untreated and electrochemically treated Pt disk electrode (f = 2000 Hz, E_L = −2.4 V and E_u = 0.8 V) in 0.5 M H_2SO_4 solution containing 0.5 M CH_3OH. In order to show the intrinsic activity (specific activity), Pt ECSA is used to normalize all the currents. The CV of the methanol electro-oxidation is characterized by two well-defined current density peaks, which reveal the classic characteristic for Pt [44, 45]. The oxidation current peak at about 0.59 V(SCE) formed during the forward CV scan corresponds to the electro-oxidation of methanol catalyzed by Pt [46, 47]. Another oxidation peak in the reverse scan at around 0.45 V(SCE) is associated with the electro-oxidation of incompletely oxidized carbonaceous species (such as CO, HCHO, and HCOOH) formed in the forward CV scan [45-47]. The current density value of the peak

formed in the forward scan (I_f) is in proportion to the amount of methanol oxidized at the electrocatalyst surface. Therefore, I_f has been generally used to characterize the electrocatalytic activity for the methanol electro-oxidation. It is seen that I_f value is almost the same for Pt disk electrodes before and after the electrochemical treatment, indicating that the electrochemical treatment doesn't obviously change the electrocatalytic activity of the Pt disk electrode for the methanol electro-oxidation. Furthermore, since the peak current in the backward CV scan (I_b) is related with the removal of adsorbed carbonaceous species obtained throughout the forward CV scan, the ratio of I_f/I_b has been extensively used to evaluate the tolerance of electrocatalyst to the poisonous carbonaceous species accumulated on the surface [47]. It is interesting to find that the electrochemical treatment of the Pt disk electrode remarkably increases the poisoning-tolerance ability of the Pt disk electrode. The value of I_f/I_b for the Pt disk electrode increases from 1.00 to 1.49 after the electrochemical treatment, indicating larger degree of methanol electro-oxidation to CO_2 and lower accumulation of poisoning carbonaceous species on the electrochemically treated Pt disk electrode surface [45, 47].
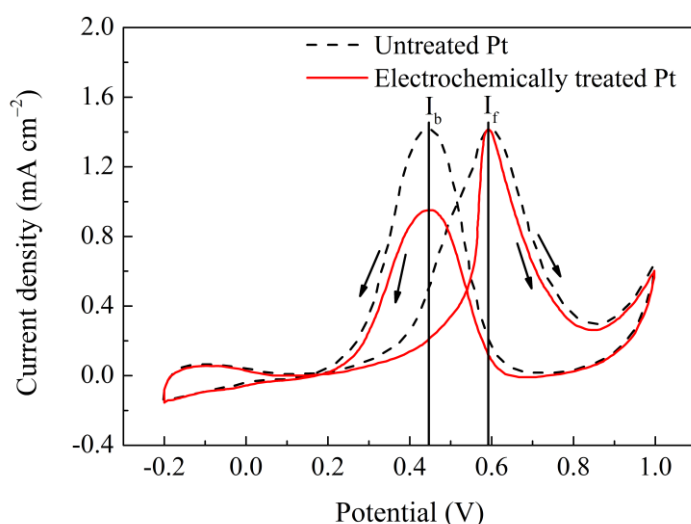

Figure 6. CVs of the methanol electro-oxidation on untreated and electrochemically treated Pt disk electrode in 0.5 M H_2SO_4 + 0.5 M CH_3OH solution at a scan rate of 0.05 V s^{-1}. All the currents are normalized by the Pt ECSA.

Fig. 7 shows CVs of the electro-oxidation of ethanol on the Pt disk electrode before and after electrochemical treatment at $f = 2000$ Hz, $E_L = -2.4$ V and $E_u = 0.8$ V. The testing solution is 0.5 M H_2SO_4 containing 0.5 M C_2H_5OH. Pt ECSA is also used to normalize both currents to better understand the intrinsic activity of the Pt electrode. In the positive scan, the current peak observed at 0.66 V(SCE) represents the electro-oxidation of the fresh ethanol on Pt surface, which is similar to that of methanol. Another current peak of oxidation recorded in the negative scan is related with the electro-oxidation of intermediate carbonaceous species produced in the positive CV scan [44]. It is worth noticing that the I_f value of electrochemically treated Pt is 3.05 times higher than that of untreated Pt disk electrode, suggesting that the electrocatalytic activity of the Pt disk electrode can be significantly improved by the electrochemical treatment. Similarly, electrochemically treated Pt exhibits much larger I_f/I_b value (2.7 times higher) than untreated Pt, indicating the increased tolerance

ability of the former against the poisoning species formed during the ethanol electro-oxidation. Since the hydrogen desorption profile shows the formation of (100)-oriented Pt surface after the electrochemical treatment (Fig. 3), the above result suggests that the Pt surface with (100) preferential orientation has higher activity than the polycrystalline surface. This agrees well with previous results reported on Pt single crystal electrodes by Colmati et al. [48], who found that the Pt(100) single crystal electrode shows the highest peak current among the three electrodes (i.e., Pt(100), Pt(111) and Pt(110) single crystal electrodes) for ethanol electro-oxidation.
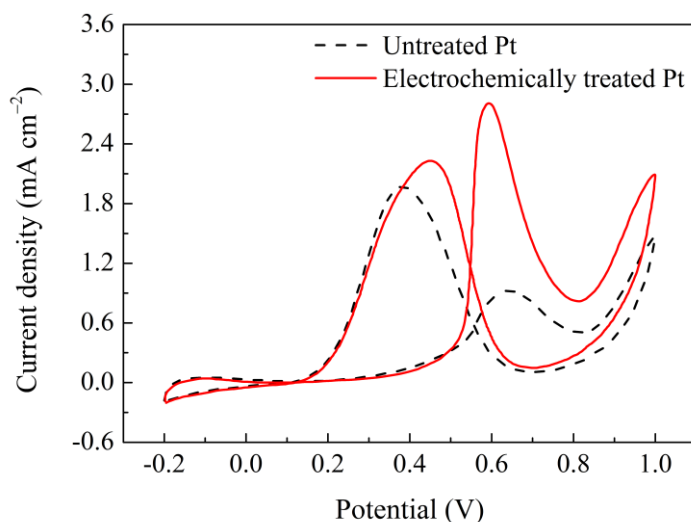

Figure 7. CVs of the ethanol electro-oxidation on untreated and electrochemically treated Pt disk electrode in 0.5 M H_2SO_4 + 0.5 M C_2H_5OH solution at a scan rate of 0.05 V s^{-1}. All the currents are normalized by the ECSA of Pt.

Fig. 8 shows CVs of the electro-oxidation of formic acid in 0.5 M H_2SO_4 + 0.5 M HCOOH for the Pt disk electrode with and without the electrochemical treatment at f = 2000 Hz, E_L = −2.4 V and E_u = 0.8 V. In the positive CV scan, a peak current density is observed at 0.66 V(SCE). In the negative CV scan, the current density increases dramatically at the beginning and then decreases sharply as the electrode potential decreases. It has been generally accepted that the electro-oxidation of formic acid on Pt electrode proceeds mainly through two pathways (i.e., direct one and indirect one). Formic acid directly oxidizes to CO_2 *via* formate or carboxylate species in the direct pathway at low potentials while poisonous CO intermediates oxidizes to CO_2 in the indirect pathway at high potentials [49-51]. It is seen that the electro-oxidation of formic acid follows the indirect oxidation pathway, showing the current peak of CO electro-oxidation at higher potential of 0.66 V(SCE) in the positive-going CV scan [50]. The relatively large current density of the peak in the negative-going scan could be attributed to the electro-oxidation of formic acid on newly reduced clean surface of Pt free of poisoning species. Tripković et al. [52] reported that the Pt(100) single crystal electrode showed less activity for formic acid electro-oxidation than the Pt(111) single crystal electrode. Sun et al. [24] also found that the electrocatalytic activity of Pt for electro-oxidation of formic acid decreases in the order of Pt(110) > Pt(111) > Pt(100). In the present work, hydrogen desorption feature shows that the electrochemical treatment results in the formation Pt surface with (100) preferential orientation and thus less Pt(111)

and Pt(110) sites compared to the untreated polycrystalline Pt disk electrode (Fig. 3). This leads to the lower activity of electrochemically treated Pt.
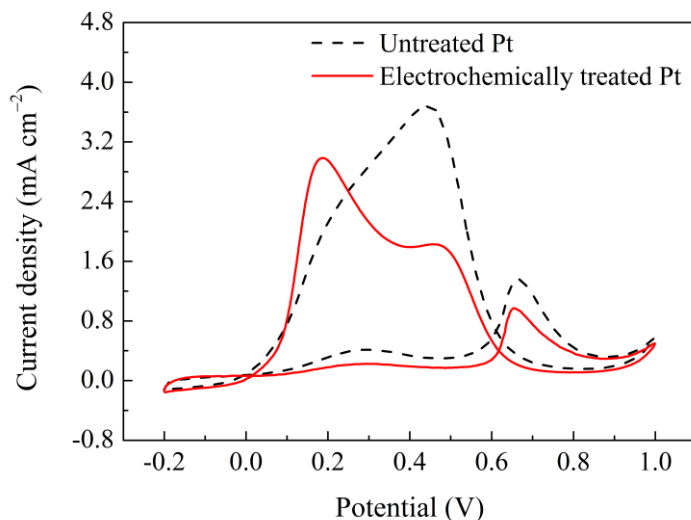

Figure 8. CVs of the formic acid electro-oxidation on untreated and electrochemically treated Pt disk electrode in 0.5 M H_2SO_4 + 0.5 M HCOOH solution at a scan rate of 0.05 V s^{-1}. All the currents are normalized by the ECSA of Pt.

To reveal the electrocatalyst activity for electro-oxidation of ammonia, Fig. 9 shows the CVs measured on untreated and electrochemically treated Pt disk electrode (f = 2000 Hz, E_L = −2.4 V and E_u = 0.8 V) in 1 M KOH + 0.05 M $(NH_4)_2SO_4$ solution. The currents are normalized by the ECSA of the Pt disk electrode. The electro-oxidation of ammonia [36, 53-55] forms a well-defined anodic current peak at around −0.34 V(SCE). Previous work from our group found that there was no such characteristic current peak when the CV was measured in KOH solution without ammonia [56]. The oxidation current peak of electrochemically treated Pt disk electrode is 0.89 mA cm^{-2}, which is 4.7 times higher than that on untreated Pt disk electrode. This suggests that the electrocatalytic activity of the Pt disk for ammonia electro-oxidation is significantly improved after the electrochemical treatment. CV measurements in H_2SO_4 solution (Fig. 3) indicate that appropriate electrochemical treatment of the Pt disk electrode results in the formation of Pt surface with (100) preferential orientation. It has been extensively reported that the ammonia electro-oxidation is very sensitive to the surface structure of Pt and it takes place almost exclusively on Pt(100) sites [35-37, 43, 57]. Therefore, the significantly improved activity of the electrochemically treated Pt disk electrode is related with the formation of increasing Pt(100) sites on the surface. It has also been found that the specific activity (activity normalized by the ECSA) of (100)-oriented Pt nanocubes is about 3–7 times higher than that reported for the polycrystalline Pt nanoparticles under the same experimental conditions [22, 37, 38, 57, 58]. The specific activity reflects the intrinsic property of electrocatalysts, depending on a series of factors such as surface crystalline orientation [38], surface morphology [59, 60] and chemical compositions [58]. The generally accepted mechanism of ammonia electro-oxidation on Pt is proposed by Gerischer and Mauerer [61]. The ammonia electro-oxidation involves the dehydrogenation of adsorbed NH_3 to partially dehydrogenated intermediates ($NH_{2,ads}$ and NH_{ads}), and fully dehydrogenated nitrogen atoms

(N_{ads}) [61]. The $NH_{2,ads}$ species are active intermediates to promote the formation of final product (N_2) while N_{ads} block the active sites of Pt surface. Both density functional theory (DFT) calculations and experimental work reveal that Pt(100) surface has high ability to stabilize active NH_2 intermediates, favoring the formation of hydrazine (N_2H_4) that is subsequently dehydrogenated quickly to N_2 [62-65]. In addition, Pt(100) has lower adsorption energy of poisoning N_{ads} compared to other crystal surfaces of Pt such as Pt(111) and Pt(110) [65]. These two factors contribute to the high specific activity of Pt(100) surface, which agrees well with the present work. The above results also evidence that the electrochemically treated Pt surface can be used as model Pt(100) electrodes to investigate the structure-sensitive electro-oxidation reactions, which significantly simplifies the preparation process to obtain (100)-oriented Pt surface.
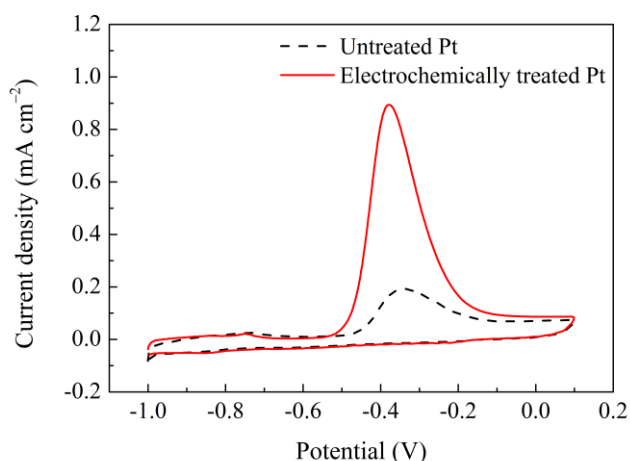

Figure 9. CVs of the ammonia electro-oxidation on untreated and electrochemically treated Pt disk electrode in 1 M KOH + 0.05 M $(NH_4)_2SO_4$ solution at a scan rate of 0.05 V s^{-1}. All the currents are normalized by the ECSA of Pt.

4. CONCLUSIONS

In the present work, the effect of the square-wave voltage on the surface orientation and the electrocatalytic activity of the Pt disk electrode with 5 mm diameter was investigated. Using two-electrode cell containing 1 M H_2SO_4 solution, Pt disk electrode with (100) preferential surface orientation was obtained by controlling the lower potential limit of –2.4 V, upper potential limit of 0.8 V and the frequency of 2000 Hz of the square-wave voltage. Hydrogen desorption profile showed the significantly increased proportion of Pt(100) sites in the electrochemically treated Pt disk electrode by the square-wave voltage. Electrochemically treated Pt disk electrodes show significantly higher specific activity for the electro-oxidation of ethanol and ammonia while lower specific activity for the electro-oxidation of formic acid compared to polycrystalline Pt electrodes. CV results of electrochemically treated Pt disk electrodes obtained in present work exhibit similar features compared to the Pt(100) single crystal electrode reported by previous studies, demonstrating that the electrochemical treatment can be used as a one-step and simple method to prepare model Pt disk electrode with (100)-oriented surface for the investigation of the structure-sensitive reactions.

References

1. R.N. Singh, R. Awasthi and C.S. Sharma, *Int. J. Electrochem. Sci.*, 9 (2014) 5607.
2. W. Ye, X. Zhang, Y. Chen, Y. Du, F. Zhou and C. Wang, *Int. J. Electrochem. S*ci., 8 (2013) 2122.
3. C. Hu, Q. Han, F. Zhao, Z. Yuan, N. Chen and L. Qu, *Science China Materials*, 58 (2015) 21.
4. R.S. Henrique, R.F.B. De Souza, J.C.M. Silva, J.M.S. Ayoub, R.M. Piasentin, M. Linardi, E.V. Spinace, M.C. Santos and A.O. Neto, *Int. J. Electrochem. Sci.*, 7 (2012) 2036.
5. F. Lopez-Garcia, G. Canche-Escamilla, A.L. Ocampo-Flores, P. Roquero-Tejeda and L.C. Ordonez, *Int. J. Electrochem. Sci.*, 8 (2013) 3794.
6. N. Erini, S. Rudi, V. Beermann, P. Krause, R. Yang, Y. Huang and P. Strasser, *ChemElectroChem*, 2 (2015) 903.
7. G.A. El-Nagar, A.M. Mohammad, M.S. El-Deab and B.E. El-Anadouli, *Int. J. Electrochem. Sci.*, 9 (2014) 4523.
8. M. Yovanovich, R.M. Piasentin, J.M.S. Ayoub, J. Nandenha, E.H. Fontes, R.F.B. de Souza, G.S. Buzzo, J.C.M. Silva, E.V. Spinace, M.H.M.T. Assumpcao, A.O. Neto and S.G. da Silva, *Int. J. Electrochem. Sci*., 10 (2015) 4801.
9. C. Zhong, W.B. Hu and Y.F. Cheng, *J. Mater. Chem. A*, 1 (2013) 3216.
10. N.J. Bunce and D. Bejan, *Electrochim. Act*a, 56 (2011) 8085.
11. F. Schüth, R. Palkovits, R. Schloegl and D.S. Su, *Energ. Environ. Sci.*, 5 (2012) 6278.
12. N.V. Rees and R.G. Compton, *Energ. Environ. Sci.*, 4 (2011) 1255.
13. C. Zhong, J. Liu, Z. Ni, Y. Deng, B. Chen and W. Hu, *Science China Materials*, 57 (2014) 13.
14. F. Vitse, M. Cooper and G.G. Botte, J. Power Sources, 142 (2005) 18.
15. M. Cooper and G.G. Botte, *J. Electrochem. Soc*., 153 (2006) A1894.
16. E.P. Bonnin, E.J. Biddinger and G.G. Botte, *J. Power Sources*, 182 (2008) 284.
17. B.K. Boggs and G.G. Botte, *J. Power Sources*, 192 (2009) 573.
18. B.K. Boggs and G.G. Botte, *Electrochim. Acta*, 55 (2010) 5287.
19. L.A. Diaz and G.G. Botte, *Electrochim. Acta*, 179 (2015) 529.
20. S.F. Xie, S. Choi, X.H. Xia and Y.N. Xia, *Curr. Opin. Chem. Eng.*, 2 (2013) 142.
21. D. Qu, Y. Tao, L. Guo, Z. Xie, W. Tu and H. Tang, *Int. J. Electrochem. Sci.*, 10 (2015) 3363.
22. F.J. Vidal-Iglesias, J. Solla-Gullon, V. Montiel, J.M. Feliu and A. Aldaz, *J. Phys. Chem. B*, 109 (2005) 12914.
23. N.M. Markovic, H.A. Gasteiger and P.N. Ross Jr, *J. Phys. Chem.,* 99 (1995) 3411.
24. S.G. Sun and Y.Y. Yang, *J. Electroanal. Chem.*, 467 (1999) 121.
25. N. Markovic, H. Gasteiger and P.N. Ross, *J. Electrochem. Soc*., 144 (1997) 1591.
26. B. Pierozynski, *Int. J. Electrochem. Sci.*, 7 (2012) 4261.
27. B. Pierozynski, *Int. J. Electrochem. Sci.*, 7 (2012) 3327.
28. S.G. Sun, A.C. Chen, T.S. Huang, J.B. Li and Z.W. Tian, *J. Electroanal. Chem.*, 340 (1992) 213.
29. R.M. Cerviño, W.E. Triaca and A.J. Arvia, J. E*lectroanal. Chem.,* 182 (1985) 51.
30. A. Visintin, J.C. Canullo, W.E. Triaca and A.J. Arvia, *J. Electroanal. Chem.*, 267 (1989) 191.
31. A. Visintin, W.E. Triaca and A.J. Arvia, *J. Electroanal. Chem.*, 221 (1987) 239.
32. A. Visintin, W.E. Triaca and A.J. Arvia, *J. Electroanal. Chem.*, 284 (1990) 465.
33. J. Gómez, L. Vázquez, A.M. Baró, N. Garcia, C.L. Perdriel, W.E. Triaca and A.J. Arvia, *Nature*, 323 (1986) 612.
34. N.M. Marković and P.N. Ross Jr, *Surf. Sci. Rep.*, 45 (2002) 117.
35. E. Bertin, S. Garbarino, D. Guay, J. Solla-Gullón, F.J. Vidal-Iglesias and J.M. Feliu, J. *Power Sources*, 225 (2013) 323.

36. S. Le Vot, L. Roué and D. Bélanger, *J. Electroanal. Chem.*, 691 (2013) 18.
37. R.A. Martínez-Rodríguez, F.J. Vidal-Iglesias, J. Solla-Gullón, C.R. Cabrera and J.M. Feliu, *J. Am. Chem. Soc.*, 136 (2014) 1280.
38. J. Liu, X.T. Du, Y. Yang, Y.D. Deng, W.B. Hu and C. Zhong, *Electrochem. Commun.*, 58 (2015) 6.
39. J.L. Zubimendi, G. Andreasen and W.E. Triaca, *Electrochim. Acta*, 40 (1995) 1305.
40. B. Lim, M. Jiang, P.H. Camargo, E.C. Cho, J. Tao, X. Lu, Y. Zhu and Y. Xia, *Science*, 324 (2009) 1302.
41. F. Gloaguen, J.M. Léger, C. Lamy, A. Marmann, U. Stimming and R. Vogel, *Electrochim. Acta*, 44 (1999) 1805.
42. K. Shimazu, D. Weisshaar and T. Kuwana, *J. Electroanal. Chem.*, 223 (1987) 223.
43. A. Ponrouch, S. Garbarino, E. Bertin, C. Andrei, G.A. Botton and D. Guay, *Adv. Funct. Mater.*, 22 (2012) 4172.
44. C.G. Hu, X.S. He and C.H. Xia, *J. Power Sources*, 195 (2010) 1594.
45. J. Liu, B. Chen, Z. Ni, Y. Deng, X. Han, W. Hu and C. Zhong, *ChemElectroChem*, DOI: 10.1002/celc.201500451 (2015).
46. H.D. Zhao, C.Z. Yu, H.J. You, S.C. Yang, Y. Guo, B.J. Ding and X.P. Song, *J. Mater. Chem.*, 22 (2012) 4780.
47. R. Mancharan and J.B. Goodenough, *J. Mater. Chem.*, 2 (1992) 875.
48. F. Colmati, G. Tremiliosi-Filho, E.R. Gonzalez, A. Berná, E. Herrero and J.M. Feliu, *Faraday Discuss.*, 140 (2008) 379.
49. Y. Kang, L. Qi, M. Li, R.E. Diaz, D. Su, R.R. Adzic, E. Stach, J. Li and C.B. Murray, *ACS Nano*, 6 (2012) 2818.
50. S. Dutta, C. Ray, A. Mondal, S.K. Mehetor, S. Sarkar and T. Pal, *Electrochim. Acta*, 159 (2015) 52.
51. A. Capon and R. Parsons, *J. Electroanal. Chem.*, 45 (1973) 205.
52. A.V. Tripković, K.D.J. Popović and J.D. Lović, *J. Serb. Chem. Soc.*, 68 (2003) 849.
53. J. Galipaud, C. Roy, M.H. Martin, S. Garbarino, L. Roué and D. Guay, *ChemElectroChem,* 2 (2015) 1187.
54. K. Yao and Y.F. Cheng, *J. Power Sources*, 173 (2007) 96.
55. K. Endo, Y. Katayama and T. Miura, *Electrochim. Acta*, 50 (2005) 2181.
56. X.H. Deng, Y.T. Wu, M.F. He, C.Y. Dan, Y.J. Chen, Y.D. Deng, D.H. Jiang and C. Zhong, *Acta Chim. Sinica*, 69 (2011) 1041.
57. J. Solla-Gullón, F.J. Vidal-Iglesias, P. Rodriguez, E. Herrero, J.M. Feliu, J. Clavilier and A. Aldaz, *J. Phys. Chem. B*, 108 (2004) 13573.
58. F.J. Vidal-Iglesias, J. Solla-Gullón, V. Montiel, J.M. Feliu and A. Aldaz, *J. Power Sources*, 171 (2007) 448.
59. J. Liu, C. Zhong, Y. Yang, Y.T. Wu, A.K. Jiang, Y.D. Deng, Z. Zhang and W.B. Hu, *Int. J. Hydrogen Energy,* 37 (2012) 8981.
60. J. Liu, W.B. Hu, C. Zhong and Y.F. Cheng, *J. Power Sources*, 223 (2013) 165.
61. H. Gerischer and A. Mauerer, *J. Electroanal. Chem.*, 25 (1970) 421.
62. V. Rosca and M.T. Koper, *Phys. Chem. Chem. Phys.,* 8 (2006) 2513.
63. V. Rosca and M.T.M. Koper, *Electrochim. Acta*, 53 (2008) 5199.
64. F. Vidaliglesias, J. Sollagullon, J. Perez and A. Aldaz, *Electrochem. Commun.*, 8 (2006) 102.
65. G. Novell-Leruth, A. Valcárcel, A. Clotet, J.M. Ricart and J. Pérez-Ramírez, *J. Phys. Chem. B*, 109 (2005) 18061.